Plasmonics
DOI 10.1007/s11468-017-0595-0

Spatial Nonlinearity in Anisotropic Metamaterial Plasmonic Slot Waveguides

Mahmoud M. R. Elsawy[1] **· Gilles Renversez**[1]

Received: 17 November 2016 / Accepted: 9 May 2017

Abstract We study the main nonlinear solutions of plasmonic slot waveguides made from an anisotropic metamaterial core with a positive Kerr-type nonlinearity surrounded by two semi-infinite metal regions. First, we demonstrate that for a highly anisotropic diagonal elliptical core, the bifurcation threshold of the asymmetric mode is reduced from the GW/m level for the isotropic case to 50 MW/m level indicating a strong enhancement of the spatial nonlinear effects. In addition, the slope of the dispersion curve for the asymmetric mode remains positive, at least near the bifurcation, suggesting a stable mode. Second, we show that for the hyperbolic case, there is no physically meaningful asymmetric mode, and that the sign of the effective nonlinearity can become negative.

Keywords Nonlinear waveguides · Plasmonics · Metamaterial · Kerr effect · Symmetry breaking · Bifurcation · Anisotropy

Introduction

Nonlinear plasmonics is now a thriving research field [1]. Its integrated branch, where surface plasmon polariton waves propagate at least partially in nonlinear media, is seen as promising in high-speed small footprint signal processing [2]. As a building block for nonlinear plasmonic circuitry, the nonlinear plasmonic slot waveguide (NPSW) is of crucial importance even in its simplest version [3, 4]. Since all the key features can be studied and understood in detail, this structure allows future generalizations from more complex linear structures like the plasmonic waveguide [5]. The strong field confinement provided by these plasmonic waveguides ensures a reinforcement of the nonlinear effects which can be boosted further using epsilon-near-zero (ENZ) materials, as was already shown [6, 7]. It is worth mentioning that metal nonlinearities have already been investigated; in one study, at least, the wavelength range of enhanced nonlinearity has been controlled using metamaterials [8]. Here, we focus on structures where the nonlinearity is provided by dielectric materials like hydrogenated amorphous silicon (a-Si:H) [9] due to its high intrinsic third-order nonlinearity around the telecommunication wavelength and to its manufacturing capabilities.

In [6], nonlinear guided waves were investigated in anisotropic structures with an isotropic effective dielectric response for transverse magnetic (TM) waves, while here, we consider a metamaterial core with an anisotropic effective dielectric response for TM waves. Other related studies [7, 8] neither focused on nonlinear waveguides nor considered plasmonic structures. The present study tackles these issues. Furthermore, a record change of 0.72 in the refractive index increase induced by a third-order nonlinearity has recently been reported for an indium tin oxide layer [10]. As concluded by the authors, this result challenges the usual hypothesis that the nonlinear term can be treated as a perturbation. One way to address this problem, for the case of nonlinear stationary waves, is to take into account the spatial profile of the fields directly from Maxwell's equations, as for example in [11, 12]. This way of proceeding is well established in studies on linear or nonlinear waveguides since the modal approach is the first key

✉ Gilles Renversez
gilles.renversez@univ-amu.fr

1 Aix–Marseille Univ, CNRS, Centrale Marseille, Institut Fresnel, Marseille, France

step [13] in investigating the self-coherent stationary states of Maxwell's equations. It has already been used many times for the study of nonlinear plasmonic structures [4, 14–17].

One of the most common phenomena in symmetric nonlinear devices including photonic ones is the symmetry breaking. It refers to the existence of solutions that do not preserve the original symmetries of the underlying system and is typically associated with a pitchfork bifurcation [18–20]; the solutions breaking the symmetry can exist only after a certain power threshold. In nonlinear optics, the symmetry breaking caused by the Kerr-type nonlinearity has been extensively studied [18, 21–23]. During the last decade, the symmetry breaking has been observed in symmetric nonlinear plasmonic waveguides composed of an isotropic nonlinear core of Kerr-type embedded between two semi-infinite metal regions at the telecommunication wavelength [4, 15, 24, 25]. The symmetry breaking in these NPSWs is associated with the emergence of an asymmetric mode which has no analogue in the linear case, and it bifurcates from the fundamental symmetric mode above a power threshold. Moreover, for the symmetric nonlinear structures with a thin nonlinear metal film surrounded by two linear dielectric regions [26], the asymmetric mode has also been observed in which the metal film presents a Kerr-like nonlinear term in its Drude dielectric response at the visible wavelength. The bifurcation of the asymmetric mode from the fundamental symmetric mode indicates a strong impact of the nonlinearity on the waveguide properties. It is a clear label of a highly nonlinear waveguide. This asymmetric mode is crucial for nonlinear optical devices and it is the key point for the power switching operation in nonlinear fiber couplers [27, 28] and for nonlinear plasmonic directional couplers composed of two adjacent symmetric NPSWs [29, 30]. These adjacent NPSWs are usually called the arms (channels) of the nonlinear directional coupler. In the nonlinear directional couplers, the optical power is coupled to one of the waveguide channels (one arm of the structure), and the output power is measured in the same waveguide channel after some distance (after all the power transfers to the second channel in a linear regime). As it is described in [29], for small input powers, the ratio between the output and the input power in the first channel (where the power is coupled) remains close to zero since all the power is transferred to the second channel. However, when the input power overcomes a fixed threshold, namely when the asymmetric mode appears, light remains mostly in the first channel providing an increase in the measured output power in this waveguide channel. The idea behind this application is the discrimination of the signals according to their power levels which cannot occur in the low power regime (before the bifurcation threshold). The interesting features in the NPSWs open even more ways to control light by light, for applications in optical signal processing in general and all-optical switching [31]. Nevertheless, it appears that the power needed to observe the interesting nonlinear effects including symmetry breaking in the symmetric NPSWs is in the range of GW/m which is still too high [4, 15, 24, 25] even for its improved version [32]. The high power level needed limits the practical implementation of such waveguides.

Here, extending to the anisotropic case the methods we have developed to study stationary states in isotropic NPSWs [16, 25], we describe the main properties obtained when a nonlinear metamaterial is used as core medium. The examples of metamaterial nonlinear cores used in the following are built applying the effective medium theory from well-known materials and realistic parameters. The main nonlinear solutions in both the elliptical and the hyperbolic case are investigated. In the first cases, we demonstrate both numerically and theoretically that for a highly anisotropic case, the effective nonlinearity [16] can be enhanced nearly up to five orders of magnitude allowing a decrease of nearly three orders of magnitude in the bifurcation threshold of the asymmetric mode existing in the symmetric structure [4, 25]. It is worth mentioning that a strong dependency of the dispersion curve on the power is observed even before the bifurcation of the asymmetric mode. In another word, at low powers, the change of the effective index becomes important (compared with its linear regime value), this is a clear indication that the nonlinear phase shift and consequently the third-order nonlinear properties like self-phase modulation, cross-phase modulation, and four-wave mixing can be extremely enhanced at low powers. These third-order nonlinear properties are crucial for all-optical signal processing.

Next, we show that, in the hyperbolic case, changes appear in the field profiles compared with those of the simple isotropic NPSWs. We also demonstrate that, due to the peculiar anisotropy, an effective defocusing effect can be obtained from the initial positive Kerr nonlinearity. In this work, we focus only on the key physical results and the used methods will be mentioned briefly. For more details about the derivation and validation of these methods, we refer to our recent technical work [33].

Model

Figure 1 shows a scheme of the nonlinear waveguide we investigate. Compared with already studied NPSWs with an isotropic nonlinear dielectric core [3, 4, 34], the new structure contains a metamaterial nonlinear core. We will study only symmetric structures even if asymmetric isotropic NPSWs have already been considered [25]. We consider monochromatic TM waves propagating along the

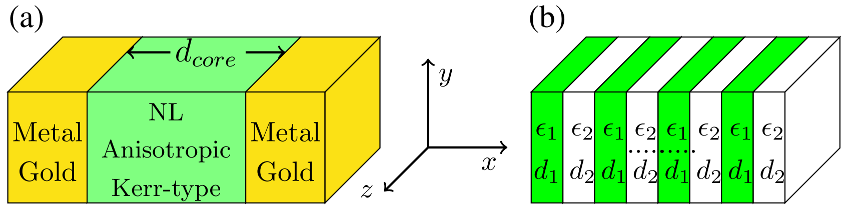

Fig. 1 **a** Symmetric NPSW geometry with its metamaterial nonlinear core and the two semi-infinite metal regions. **b** Metamaterial nonlinear core obtained from a stack of two types of layers with permittivities and thicknesses ε_1 and d_1 and ε_2 and d_2, respectively. Only material 1 is nonlinear

z direction (all field components evolve proportionally to $\exp[i(k_0 n_{eff} z - \omega t)]$) in a one-dimensional NPSW depicted in Fig. 1. Here, $k_0 = \omega/c$, where c denotes the speed of light in vacuum, n_{eff} denotes the effective mode index and ω is the light angular frequency. The electric field components are $(E_x, 0, iE_z)$ and the magnetic field is $(0, H_y, 0)$. In all the waveguide, the magnetic permeability is equal to μ_0, that of vacuum. The nonlinear Kerr-type metamaterial core of thickness d_{core} is anisotropic (see Fig. 1). Its full effective permittivity tensor $\bar{\bar{\varepsilon}}_{eff}$ has only three non-null diagonal terms. Its linear diagonal elements are ε_{jj} $\forall j \in \{x, y, z\}$. We derive these terms from simple effective medium theory (EMT) applied to a stack of two isotropic material layers. d_1 and d_2 are the layer thicknesses of isotropic material 1 (nonlinear, of focusing Kerr-type) and material 2 (linear), respectively. Their respective linear permittivities are ε_1 and ε_2. The EMT is typically valid when the light wavelength λ is much larger than d_1 and d_2. Depending on the chosen orientation of the compound layers relative to the Cartesian coordinate axes, different anisotropic permittivity tensors can be built for the core. Due to the required z-invariance, only two tensor types, where the z-axis belongs to the layers, have to be considered. For the first one where the layers are parallel to the x-axis, one has, for the linear diagonal terms of $\bar{\bar{\varepsilon}}_{eff}$: $[\varepsilon_{xx} = \varepsilon_{//} \;\; \varepsilon_{yy} = \varepsilon_{\perp} \;\; \varepsilon_{zz} = \varepsilon_{//}]$ with $\varepsilon_{//} = \Re e(r\varepsilon_2 + (1-r)\varepsilon_1)$, $\varepsilon_{\perp} = \Re e((\varepsilon_1\varepsilon_2)/(r\varepsilon_1 + (1-r)\varepsilon_2))$, and $r = d_2/(d_1 + d_2)$. For the second case where the layers are parallel to the y-axis (see Fig. 1b), one gets: $[\varepsilon_{\perp} \;\; \varepsilon_{//} \;\; \varepsilon_{//}]$. We will focus only on this second case. In this study, only the real parts of the material permittivities will be considered since we are interested only in determining the effective indices of the propagating waves. The presence of losses in the considered metamaterials is unavoidable and mainly depends on the imaginary parts of its constituent materials with permittivities ϵ_1 and ϵ_2. Nevertheless, the loss problem can be alleviated by incorporating gain medium in the core. Numerous theoretical [35–38] and experimental [39, 40] studies have already introduced an active medium to compensate for the losses in structures based on layered metamaterials.

To model these anisotropic waveguides, we assume that the nonlinear Kerr term is isotropic. The j-th component of the full effective permittivity tensor, $\varepsilon_{eff,j} = \varepsilon_{jj} + \tilde{\alpha}(E_x^2 + E_z^2)$ with $\tilde{\alpha} = \varepsilon_0 c \Re e(\varepsilon_1)(1-r) n_{2,1}$ where $n_{2,1}$ is the nonlinear coefficient of the material 1, and is set at $2.10^{-17} m^2/W$ as used in [25]. This is an approximation compared with the full treatment of the anisotropic nonlinearity [33, 41]. To tackle the full case is beyond the scope of our study, which is mostly dedicated to the impact of the anisotropy of the linear terms (its extension, though, can be seen as what the next step should be in this research field). In this study, the wavelength is 1.55 μm. The permittivity of material 1, ε_1 (corresponding to a-Si:H), and the permittivity of the gold metal claddings (see Fig. 1a) are the same as in [32], while d_{core} is fixed at 400 nm (except in Fig. 2). Next, the two used models of the Kerr nonlinear field dependence are described.

In the first model, only the transverse component of the electric field E_x, which is usually larger than the longitudinal one is taken into account. This approximation

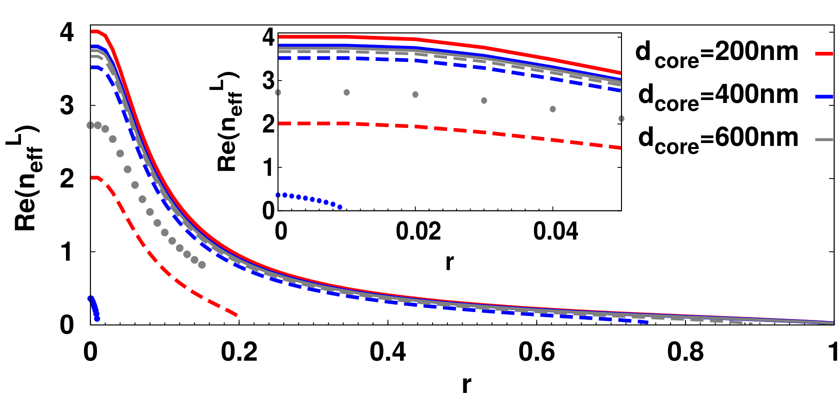

Fig. 2 Linear dispersion curves for symmetric NPSWs as a function of r parameter in the elliptical case for three different core thicknesses d_{core} with $\varepsilon_2 = 1.0\,10^{-5} + i0.62$. *Solid lines* stand for first symmetric modes, *dashed lines* for first antisymmetric modes, and points for first higher-order symmetric modes. *Inset*: zoom for the region near $r = 0$

has already been used for several models of isotropic NPSWs [16, 32, 34]. Its results are similar to those of more accurate approaches where all the electric field components are considered in the optical Kerr effect [16, 34]. This first model allows to use our new semi-analytical approach called EJEM (for Extended Jacobi Elliptical Model, which is an extension to the anisotropic case [33] of our previously developed JEM valid for isotropic configurations [16]). This approach will provide insights into the effective nonlinearity dependence on the opto-geometric parameters. This approximation for the nonlinear term also allows to use the simple fixed power algorithm in the finite element method (FEM) to compute the nonlinear stationary solutions and their nonlinear dispersion curves [12, 14, 42, 43] in order to validate our EJEM results.

In the second model, all the electric field components are considered in the nonlinear term, and we need to use the more general FEM approach we developed [33] to generalize the one-component fixed power algorithm [34] in such structures.

Results for the Elliptical Case

Now, we investigate the elliptical case for the metamaterial nonlinear core such that $\varepsilon_{xx} > 0$ and $\varepsilon_{zz} > 0$. For material 2 in the core, we choose an ENZ material such that $\varepsilon_2 = 1.0\,10^{-5} + i0.62$ being similar to the one provided in [44]. We start this study with the linear case in which the main linear modes we found are of plasmonic type. For the metamaterial core, besides the permittivities, we have the ratio r defined above as new degree of freedom. As a result, one can obtain linear dispersion curves as a function of r. Figure 2 shows such curves for several values of the core thickness d_{core}. n^L_{eff} indicates n_{eff} of the linear case. One can see that it is possible to choose configurations where only the first symmetric mode is kept. This kind of behavior can be an advantage to achieve simpler and better control of nonlinear propagating solutions as a function of power [45] or to tune the linear dispersion properties as a function of wavelength to manage the dispersion coefficients. As a test signature for strong nonlinear spatial behavior and a demanding validity check, we depict the Hopf bifurcation of the symmetric mode toward the asymmetric mode in symmetric isotropic and anisotropic NPSWs. In Fig. 3, we provide the results obtained with the methods we used, the EJEM and the two FEMs without and with all the electric field components in the nonlinear term. For comparison with this latter case, we also use the interface model (IM) we developed previously to study the isotropic case taking into account all the electric field components [16].

First for the isotropic case (Fig. 3a), the FEM taking into account only the electric field transverse component (cyan curves) is able to recover the results from the EJEM (blue

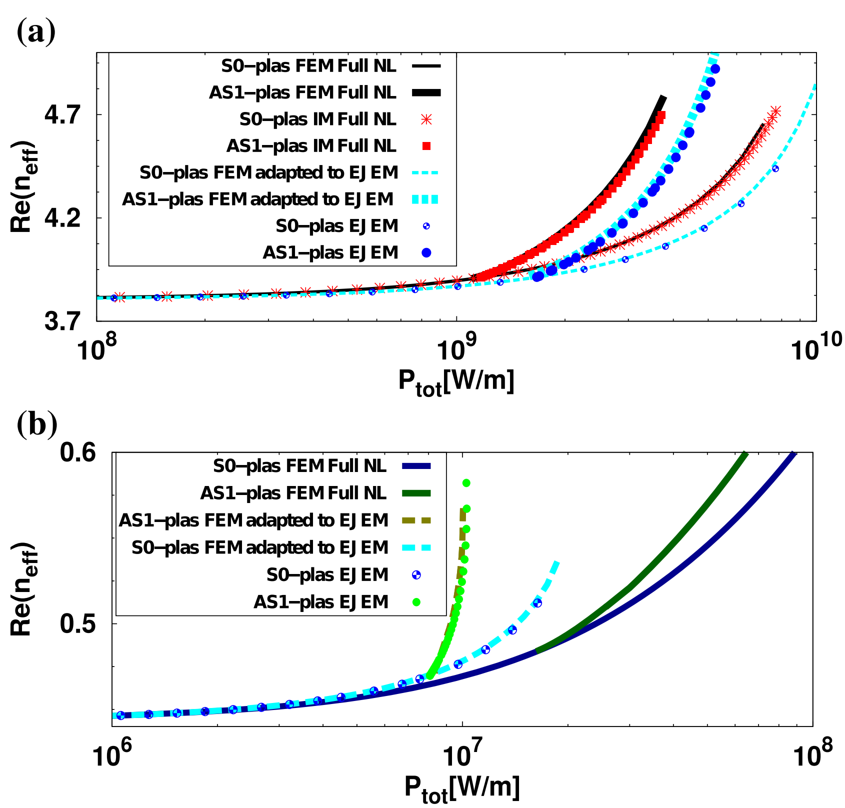

Fig. 3 Nonlinear dispersion curves for symmetric NPSWs as a function of total power P_{tot}. Both the symmetric modes (*bottom branch for each color*) denoted S0-plas and the asymmetric ones AS1-plas (*upper branch after bifurcation*) are shown, the mode notation is fully coherent with the ones used for the simple [16, 25] or improved [32] isotropic NPSWs. **a** Isotropic case ($r = 0$) with the EJEM, the FEM with and without all the electric field components in the nonlinear term, and the IM. **b** Elliptical anisotropic case ($r = 0.35$) with the EJEM, and the two FEMs

curves), and our FEM with both electric field components (black curves) reproduces the results obtained from the IM (red curves). Second, for the anisotropic case (Fig. 3b), EJEM and FEM agree well with one another. As expected, the results for FEM with and without all the electric field components in the nonlinear term differ slightly at high powers. Consequently, these results prove the validity of our numerical methods for nonlinear studies including the anisotropic case (for more details about our two new methods the reader can relate to Ref. [33]).

In Fig. 4, we provide the field profiles for the three non-null electromagnetic field components for the anisotropic case with $r = 0.35$ at two different power values. These field profiles correspond to the symmetric S0-plas mode and the asymmetric AS1-plas mode depicted in Fig. 3b. The asymmetric mode AS1-plas bifurcates from the nonlinear symmetric mode S0-plas at a critical power value $P_{tot} \approx 1.6 \times 10^7$ W/m. Moreover, this mode tends to be more localized at one of the interfaces with the increase of the power as it can be seen in Fig. 4. It is worth mentioning that the field profiles obtained in the anisotropic elliptical case are similar to the ones already found in the isotropic case with $r = 0$ [25]. Nevertheless, due to the anisotropy, we can drastically reduce the bifurcation threshold and make it as low as the 50 MW/m level (see Fig. 3b).

Despite the enhancement of nonlinear effects due to the use of ENZ materials demonstrated both theoretically [6–8] and experimentally [10], Fig. 5 shows that, in the isotropic case, the ENZ material core does not reduce the bifurcation threshold but increases it. This can be understood qualitatively as follows. In ENZ material the wavelength light is stretched, thus the two core interfaces are more tightly coupled and more power is needed by the nonlinearity to break the symmetry of the field profile. In the anisotropic case, as it can be seen in Figs. 3b and 6, considering a nonlinear core with ENZ ε_{xx} and large ε_{zz} allows the total power needed to induce symmetry breaking in NPSWs to be drastically reduced compared with what is needed in the isotropic case. As a result, the threshold is shifted from the GW/m level to approximately 50 MW/m. Using our semi-analytical

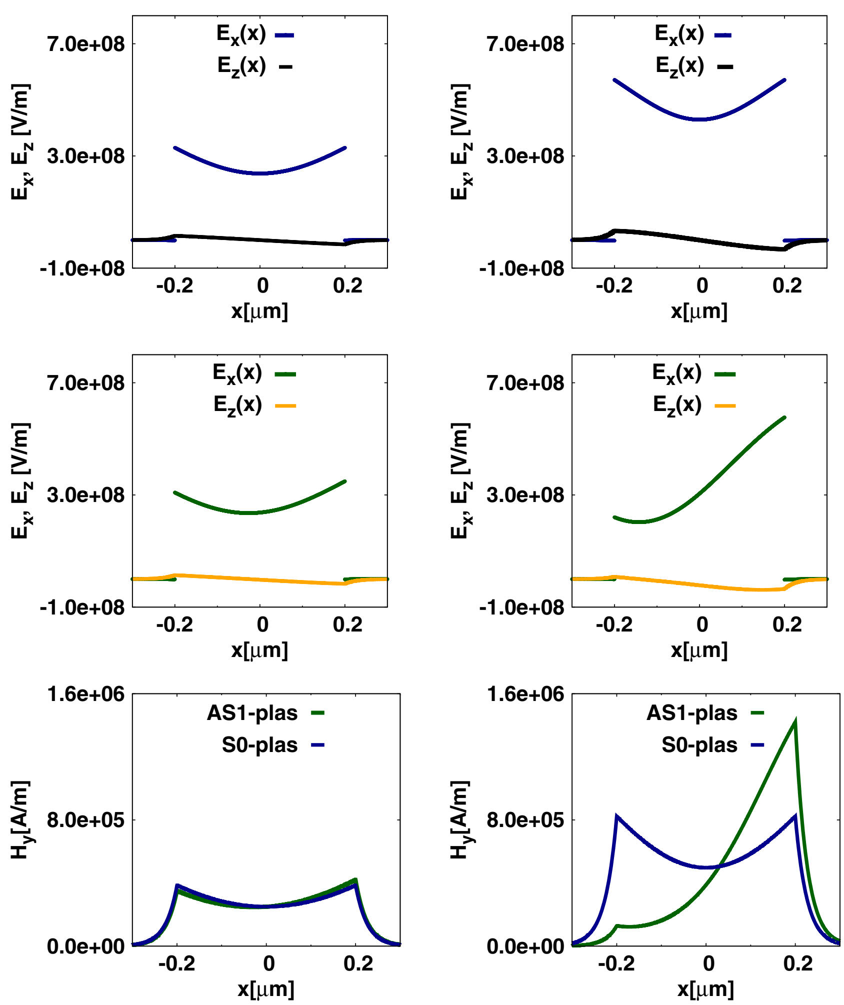

Fig. 4 The field profiles in the anisotropic elliptical case with $r = 0.35$ at two different power values. The first column is obtained for $P_{tot} = 1.62 \times 10^7$ W/m while the second column for $P_{tot} = 5.99 \times 10^7$ W/m. The *first* and *the second rows* represent the electric field components for the symmetric mode S0-plas and the asymmetric mode AS1-plas, respectively. The *third row* corresponds to the magnetic field profile H_y for both the symmetric (*dark-blue*) and the asymmetric (*dark-green*). These field profiles are computed using our FEM taking into account the full treatment of the Kerr nonlinearity

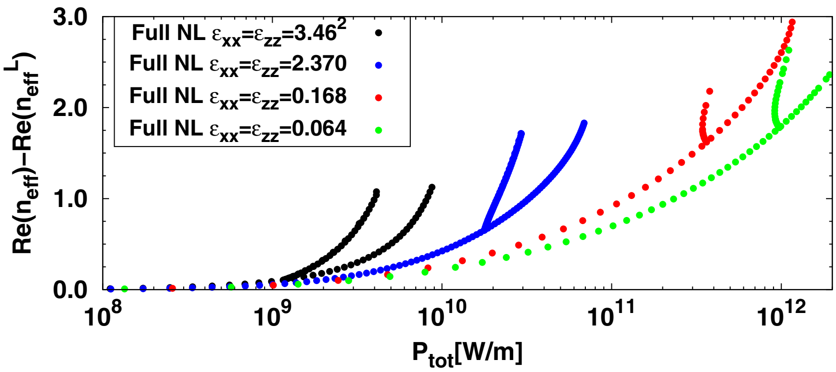

Fig. 5 Nonlinear dispersion curves for isotropic symmetric NPSWs as a function of total power P_{tot} and for different values of linear core permittivity. Both the symmetric modes and the asymmetric ones are shown. The *curves* have been translated along the y-axis to improve visibility, n_{eff}^L representing the effective index n_{eff} in the linear case

EJEM, we obtain the following analytical expression for the effective nonlinearity term [16] in the studied anisotropic NPSWs [33]:

$$a_{nl}^{\text{EJEM}} = \frac{-\tilde{\alpha}[\Re e(n_{eff})]^2}{\varepsilon_{xx}^4 c^2 \varepsilon_0^2}\left([\Re e(n_{eff})]^2 \left(\varepsilon_{xx} - \varepsilon_{zz}\right) - \varepsilon_{xx}^2\right). \tag{1}$$

Consequently, for the NPSWs, the reinforcement of the effective nonlinearity with ENZ ε_{xx} and large ε_{zz} is clearly understood and quantified. It seems to have been partially overlooked in some previous studies, due to the fact that more attention was dedicated to the permittivity tensor case one $[\varepsilon_{//} \;\; \varepsilon_{\perp} \;\; \varepsilon_{//}]$ leading to $\varepsilon_{xx} = \varepsilon_{zz} = \varepsilon_{//}$, and not the case two, as studied here with $[\varepsilon_{\perp} \;\; \varepsilon_{//} \;\; \varepsilon_{//}]$ leading to non-vanishing terms in Eq. 1. The observed reduction of the bifurcation threshold is not possible either in isotropic improved NPSWs [32] or in isotropic ENZ NPSWs, as shown in Fig. 5. Figure 7 gives the bifurcation thresholds as a function of transverse and longitudinal permittivities for several configurations. Above the black line associated with the isotropic case, the thresholds are higher while they are smaller below. In the anisotropic case, for ENZ ε_{xx}, one can see the strong decrease in threshold. For a fixed ε_{xx}, an increase in ε_{zz} induces a decrease in the bifurcation threshold (see inset in Fig. 7).

Nevertheless, it can be argued that threshold decreases of several orders of magnitude have already been predicted [16, 25], but this result was obtained using a large increase of the core size, shifting the structure from nanophotonics to large integrated optics structures. In the present case, small core thicknesses can be kept, allowing not only a limited footprint for the devices but also a limited number of propagating modes in the metamaterial based NPSWs, possibly only the fundamental symmetric mode (see Fig. 2) and the associated asymmetric one. One can also notice that the dispersion curve slopes of the symmetric nonlinear mode, for the highly anisotropic NPSWs studied, are not negligible even below the reduced bifurcation threshold, involving important nonlinear effects on the propagation of this mode even at lower powers. Another consequence of the use of a highly anisotropic elliptical metamaterial core is the low value of the effective indices for the main modes (see Fig. 3b), ensuring a slow light enhancement for the nonlinear effects in temporal propagation configurations [46]. The

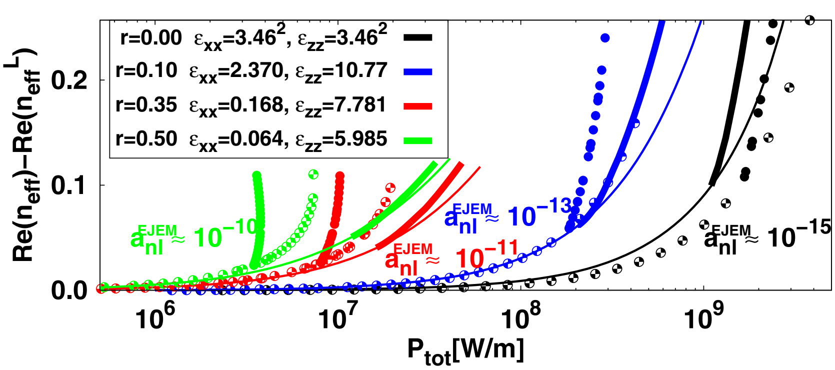

Fig. 6 Nonlinear dispersion curves for elliptical anisotropic and isotropic symmetric NPSWs as a function of the total power P_{tot} for different values of the ratio r. Both the symmetric modes and the asymmetric ones are shown. The *curves* have been translated along the y-axis to improve visibility. The associated values of the effective nonlinearity a_{nl}^{EJEM} at the bifurcation threshold are also given. The *solid curves* have been obtained with the full FEM while the *circles* have been obtained with the EJEM

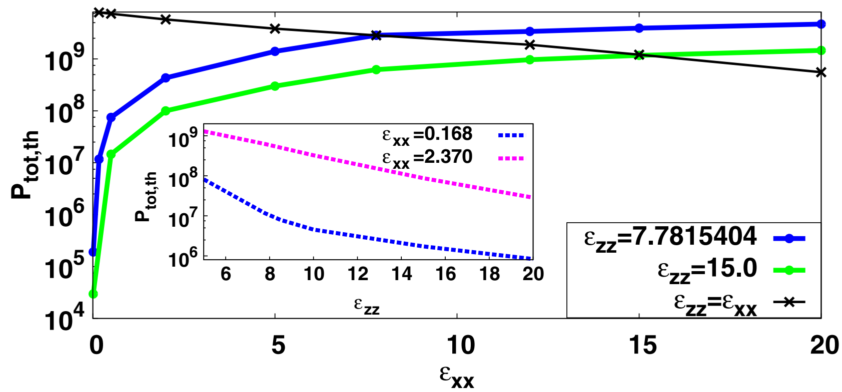

Fig. 7 Power at the bifurcation threshold $P_{tot,th}$ as a function of linear transverse permittivity ε_{xx} in the elliptical case for two longitudinal permittivity ε_{zz} values. Isotropic case is shown by the *black curve*. *Inset*: $P_{tot,th}$ as a function of ε_{zz} for two ε_{xx} values

impact of the core anisotropy is also seen on the dispersion curve of the main asymmetric mode. As shown in Fig. 5 (isotropic case), the lower the core permittivity, the larger the slope of the asymmetric mode branch. Moreover, for ENZ isotropic cores ($\varepsilon_{core} \lesssim 1$), the slope is negative while, as shown in Fig. 6, for highly anisotropic cores with ENZ ε_{xx} and large ε_{zz}, the slope of the asymmetric mode near the bifurcation point remains positive. If we assume that the stability results we obtained for isotropic NPSWs [25] can be extended to the anisotropic case, these two features suggest that the asymmetric mode should be unstable in isotropic ENZ core NPSWs ($\varepsilon_{core} \lesssim 1$) while the same mode should be stable for highly anisotropic core with ENZ ε_{xx} and large ε_{zz} (a full stability study of the main modes as described in [25] for simple NPSWs is beyond the scope of this study). To conclude this discussion of the elliptical case, we can notice that if the nonlinearity of the ENZ material [7, 10] used for material 2 was taken into account then the effective nonlinearity of the full core would increase, and consequently the bifurcation threshold would be further reduced compared to the configuration we described.

Results for the Hyperbolic Case

We now investigate the hyperbolic case where the metamaterial core is such that $\varepsilon_{xx} > 0$ and $\varepsilon_{zz} < 0$. In this case, it is known that non-local effects can be neglected in EMT as soon as the condition $d_1 = d_2$ is fulfilled, corresponding to $r = 0.5$ [47]. We will limit our study to such configurations. generate this case, material 2 in the core is now copper [48] while material 1 is hydrogenated amorphous silicon [9] and the claddings are made of gold as in all our study; the wavelength being fixed at 1.55 μm like in the previous case. Linear studies of waveguides involving similar linear metamaterial core have already been published [49]. For NPSWs, we found that the main modes are core localized unlike those of simple NPSWs, and that the effective nonlinearity can be negative for the investigated modes, meaning that the initial positive Kerr nonlinearity can finally act as a negative one in such anisotropic configuration. This can be understood looking at Eq. 1. Figure 8 illustrates this phenomenon.

We also found that the asymmetric mode we can obtain as a mathematical solution to the nonlinear dispersion equation is actually unbounded [33], knowing that similar unbounded modes have already been obtained in other nonlinear structures [50]. Therefore, this asymmetric mode cannot be considered as an acceptable solution to our physical problem. The nonlinear dispersion curves of the main symmetric and antisymmetric modes are given in Fig. 9. Once again, one can see the crucial influence of the metamaterial core properties on the type and behavior of the propagating nonlinear solutions. It is worth mentioning that the nonlinearity of noble metal can be neglected at the telecommunication wavelength, while it is not the case in the visible as it can be seen in [8].

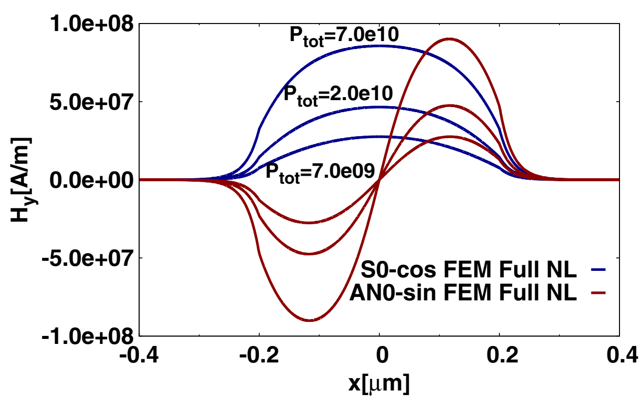

Fig. 8 Hyperbolic symmetric NPSWs for $\varepsilon_{xx} = 26.716$ and $\varepsilon_{zz} = -51.514$ (obtained from material 2 permittivity $\varepsilon_2 = -115 + i6$ (copper [48]) and $r = 0.5$). For $\tilde{\alpha}$ (See the second paragraph of Section "Model". Field profiles $H_y(x)$ for the main symmetric (S0-cos) and antisymmetric (AN0-sin) modes as a function of total power P_{tot} (in W/m)

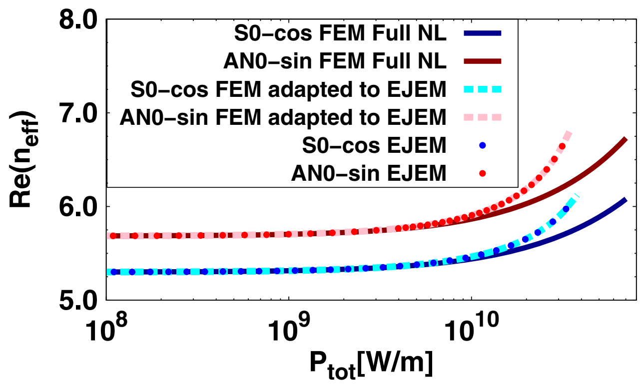

Fig. 9 Hyperbolic symmetric NPSWs for the same parameters as in Fig. 8: $\varepsilon_{xx} = 26.716$ and $\varepsilon_{zz} = -51.514$, and r=0.5. Nonlinear dispersion *curves* as a function of P_{tot}. The curves for the main symmetric (S0-cos) and antisymmetric (AN0-sin) modes are shown for both the EJEM and the two FEMs

Conclusion

We have studied new NPSWs with an anisotropic metamaterial nonlinear core of positive Kerr-type embedded between two semi-infinite metal claddings. The found spatial nonlinear effects are a signature of a strong nonlinear reinforcement. The GW/m bifurcation threshold needed in the isotropic cases [25], even in improved NPSWs [32], is lowered to tens of MW/m for elliptical anisotropic NPSWs with ENZ ε_{xx} and large ε_{zz}. This improvement makes the properties of the proposed waveguides really attainable for materials used in current fabrication processes in photonics and also to most characterization setups. For hyperbolic anisotropic NPSWs, the effective nonlinearity can change its sign passing from a focusing nonlinearity to a defocusing one.

Acknowledgements G. R. would like to thank the PhD school ED 352 “Physique et Sciences de Matière” and the International Relation Service of Aix-Marseille University (project AAP 2015 ”Noliplasmo 2D”) for their respective fundings.

References

1. Kauranen M, Zayats AV (2012) Nat Photon 6:737
2. Melikyan A, Alloatti L, Muslija A, Hillerkuss D, Schindler PC, Li J, Palmer R, Korn D, Muehlbrandt S, Thourhout DV, Chen B, Dinu R, Sommer M, Koos C, Kohl M, Freude W, Leuthold J (2014) Nat Photon 8:229
3. Feigenbaum E, Orenstein M (2007) Opt Lett 32(6):674
4. Davoyan AR, Shadrivov IV, Kivshar YS (2008) Opt Express 16(26):21209
5. Oulton RF, Sorger VJ, Genov DA, Pile DFP, Zhang X (2008) Nat Photon 2:496. doi:10.1038/nphoton.2008.131. http://www.nature.com/nphoton/journal/v2/n8/suppinfo/nphoton.2008.131_S1.html
6. Ciattoni A, Rizza C, Palange E (2010) Phys Rev A 81(4):043839. doi:10.1103/PhysRevA.81.043839
7. Ciattoni A, Rizza C, Marini A, Di Falco A, Faccio D, Scalora M (2016) Laser Photon Rev 10(3):517. doi:10.1002/lpor.201500326
8. Neira AD, Olivier N, Nasir ME, Dickson W, Wurtz GA, Zayats AV (2015) Nat Commun 6:7757. doi:10.1038/ncomms8757
9. Lacava C, Minzioni P, Baldini E, Tartara L, Fedeli JM, Cristiani I (2013) Appl Phys Lett 103(14):141103
10. Alam MZ, De Leon I, Boyd RW (2016) Science 352(6287):795. doi:10.1126/science.aae0330. http://science.sciencemag.org/content/352/6287/795
11. Snyder AW, Mitchell DJ, Chen Y (1994) Opt Lett 19(8):524
12. Drouart F, Renversez G, Nicolet A, Geuzaine C (2008) J Opt A: Pure Appl Opt 10(12):125101
13. Snyder AW, Mitchell DJ, Poladian L (1991) J Opt Soc Am B 8(8):1618. doi:10.1364/JOSAB.8.001618. http://josab.osa.org/abstract.cfm?URI=josab-8-8-1618
14. Walasik W, Renversez G, Kartashov YV (2014) Phys Rev A 89(2):023816
15. Salgueiro JR, Kivshar YS (2014) J Opt 16(11):114007. http://stacks.iop.org/2040-8986/16/i=11/a=114007
16. Walasik W, Renversez G (2016) Phys Rev A 93:013825. doi:10.1103/PhysRevA.93.013825
17. Ajith R, Mathew V (2015) Opt Commun 346:183
18. Akhmediev N (1982) Sov Phys JETP 56:299
19. Bulgakov E, Sadreev A (2011) J Phys Cond Matter 23(31):315303
20. Torres JP, Boyce J, Chiao RY (1999) Phys Rev Lett 83:4293. doi:10.1103/PhysRevLett.83.4293
21. Soto-Crespo JM, Akhmediev N (1993) Phys Rev E 48:4710. doi:10.1103/PhysRevE.48.4710
22. Peschel T, Peschel U, Lederer F (1994) Phys Rev A 50:5153. doi:10.1103/PhysRevA.50.5153
23. Xu Y, Coen S (2014) Opt Lett 39(12):3492. doi:10.1364/OL.39.003492. http://ol.osa.org/abstract.cfm?URI=ol-39-12-3492
24. Rukhlenko ID, Pannipitiya A, Premaratne M, Agrawal G (2011) Phys. Rev. B 84(11):113409
25. Walasik W, Renversez G, Ye F (2016) Phys. Rev. A 93:013826. doi:10.1103/PhysRevA.93.013826
26. Davoyan AR, Shadrivov IV, Kivshar YS (2011) Opt Lett 36(6):930
27. Chu PL, Malomed BA, Peng GD (1993) J Opt Soc Am B 10(8):1379. doi:10.1364/JOSAB.10.001379. http://josab.osa.org/abstract.cfm?URI=josab-10-8-1379
28. Maes B, Soljačić M, Joannopoulos JD, Bienstman P, Baets R, Gorza SP, Haelterman M (2006) Opt Express 14(22):10678. doi:10.1364/OE.14.010678. http://www.opticsexpress.org/abstract.cfm?URI=oe-14-22-10678
29. Salgueiro JR, Kivshar YS (2010) Appl Phys Lett 97(8):081106. doi:10.1063/1.3482939. http://aip.scitation.org/doi/abs/10.1063/1.3482939
30. Kusko C (2012) In: CAS 2012 (International semiconductor conference), vol 1, pp 143–146. doi:10.1109/SMICND.2012.6400673
31. Nozhat N, Granpayeh N (2014) Appl Opt 53(15):3328. doi:10.1364/AO.53.003328. http://ao.osa.org/abstract.cfm?URI=ao-53-15-3328
32. Elsawy MMR, Renversez G (2016) Opt Lett 41(7):1542. doi:10.1364/OL.41.001542. http://ol.osa.org/abstract.cfm?URI=ol-41-7-1542
33. Elsawy MMR, Renversez G (2017) J Opt doi:10.1088/2040-8986/aa7094
34. Walasik W, Rodriguez A, Renversez G (2015) Plasmonics 10:33
35. Smalley JST, Vallini F, Kanté B., Fainman Y (2014) Opt Express 22(17):21088. doi:10.1364/OE.22.021088. https://www.osapublishing.org/oe/abstract.cfm?uri=oe-22-17-21088
36. Savelev RS, Shadrivov IV, Belov PA, Rosanov NN, Fedorov SV, Sukhorukov AA, Kivshar YS (2013) Phys Rev B 87(11):115139. doi:10.1103/PhysRevB.87.115139

37. Argyropoulos C, Estakhri NM, Monticone F, Alù A (2013) Opt Express 21(12):15037. doi:10.1364/OE.21.015037. https://www.osapublishing.org/oe/abstract.cfm?uri=oe-21-12-15037
38. Smalley JST, Vallini F, Shahin S, Kanté B., Fainman Y (2015) Opt Mat Express 5(10):2300. doi:10.1364/OME.5.002300. https://www.osapublishing.org/abstract.cfm?URI=ome-5-10-2300
39. Rizza C, Di Falco A, Ciattoni A (2011) Appl Phys Lett 99(22):221107. doi:10.1063/1.3665414. http://scitation.aip.org/content/aip/journal/apl/99/22/10.1063/1.3665414
40. Grandidier J, des Francs GC, Massenot S, Bouhelier A, Markey L, Weeber JC, Finot C, Dereux A (2009) Nano Lett 9(8):2935. doi:10.1021/nl901314u
41. Boyd RW (2007) Nonlinear optics. Academic, New York
42. Rahman BMA, Souza JR, Davies JB (1990) IEEE Photon Technol Lett 2(4):265
43. Ferrando A, Zacarés M, de Cordoba PF, Binosi D, Monsoriu JA (2003) Opt Express 11(5):452
44. Capretti A, Wang Y, Engheta N, Negro LD (2015) Opt Lett 40(7):1500. doi:10.1364/OL.40.001500. http://ol.osa.org/abstract.cfm?URI=ol-40-7-1500
45. Akhmediev N, Ankiewicz A (1997) Solitons, nonlinear pulses and beams. Chapman & Hall, London
46. Baba T (2008) Nat Photon 2(8):465. http://search.ebscohost.com.gate1.inist.fr/login.aspx?direct=true&db=a9h&AN=33380543&lang=fr&site=ehost-live
47. Chebykin AV, Orlov AA, Vozianova AV, Maslovski SI, Kivshar YS, Belov PA (2016) Phys Rev B 84(11):115438. doi:10.1103/PhysRevB.84.115438
48. Fedyanin DY, Yakubovsky DI, Kirtaev RV, Volkov VS (2016) Nano Lett 16(1):362. doi:10.1021/acs.nanolett.5b03942
49. Avrutsky I, Salakhutdinov I, Elser J, Podolskiy V (2007) Phys Rev B 75(24):241402. doi:10.1103/PhysRevB.75.241402
50. Chen W, Maradudin AA (1988) J Opt Soc Am B 5(2):529